A Comprehensive Modeling of Vehicle-To-Vehicle Based VLC System under Practical Considerations, an Investigation of Performance, and Diversity Property

Pranav Sharda, *Student Member, IEEE,* Gundala S. Reddy, *Student Member, IEEE,* Manav R. Bhatnagar, *Senior Member, IEEE*, and Zabih Ghassemlooy, *Senior Member, IEEE, Fellow of OSA*

Abstract

In this work, a vehicle-to-vehicle (V2V) visible light communications (VLC) model for two **practical scenarios**, is proposed. In scenario 1, the random lateral shift of vehicles and the deterministic longitudinal separation between two communicating vehicles are considered, whereas in scenario 2, longitudinal separation between two vehicles is considered to be random, and lateral shift of vehicles is considered to be deterministic. To this end, we emphasize **comprehensive modeling** of the **practical characteristics** of the considered V2V-VLC system, such as **random path loss** due to the **random mobility** of the vehicle, **random lateral shift** and **random longitudinal separation** of the vehicle. Moreover, we analyze the performance of the proposed V2V-VLC model in terms of different metrics under the consideration of a **novel channel model**. Considering our **findings**, it is observed that the random lateral shift of the vehicle and the random longitudinal separation between two vehicles have a significant impact on the V2V-VLC system performance. Further, at a distance of 40 m, for example, the path loss **penalties** for moderate and dense fog weather scenarios are 2 and 3 dB, respectively, compared with the clear weather. Furthermore, the **combined impact** of path loss and atmospheric turbulence affects the V2V-VLC performance significantly.

Pranav Sharda, Gundala S. Reddy, and Manav R. Bhatnagar are with the Department of Electrical Engineering, Indian Institute of Technology Delhi, Hauz Khas, New Delhi 110016, India. Z. Ghassemlooy is with the Optical Communications Research Group, School of Computing, Engineering and Information Sciences, Northumbria University, Newcastle upon Tyne, NE1 8ST, U.K. E-mails: shardapranav73@gmail.com,Gundala.Sujith.Reddy.eee19@ee.iitd.ac.in, manav@ee.iitd.ac.in, z.ghassemlooy@northumbria.ac.uk .

Index Terms

average bit error rate (ABER), visible light communications (VLC), vehicle-to-vehicle (V2V).

I. Introduction

A. Background and State-of-the-Art

For supporting next-generation high-speed wireless communication systems, along with other emerging fifth-generation (5G) technologies such as network densification, millimeter-wave (mm-Wave), and massive multiple-input multiple-output (MIMO), visible light communications (VLC) have attracted significant attention in both academia and industry [1]. Contrary to the radio frequency (RF) communications technology, VLC systems are free from spectrum licensing [2]. Moreover, due to the spatial confinement of optical beams, it offers higher data rates and improved security. As compared to the existing RF systems, the absence of RF-induced electromagnetic interference in the VLC systems makes it a promising technology [2]. Further, VLC systems, which employ light-emitting diode (LED), are energy-efficient, low-cost, and offer a satisfactory area spectral efficiency (ASE) [3]. Since LEDs can switch faster than the human eye can respond, they can be intensity modulated at higher data rates, thus offering simultaneous illumination and communication capabilities [4]. To this end, nowadays, VLC is considered one of the most vital green communication technologies [5]. Due to the full compatibility of VLC with RF communications, the two can complement each other, forming hybrid networks and thus enhancing the communication performance as well [6]. Contrary to other wireless communication technologies, VLC is safe for human health, provided the illumination level is below the eye safety level. Furthermore, VLC systems do not affect the functionality of the highly-sensitive electronic systems, and thus, can be used in RF restricted places (e.g., airplanes, hospitals, chemical or nuclear plants) [7].

As far as the indoor environment is concerned, VLC systems have been investigated, considering modulations [8], coding [9], MIMO [10], spectrally efficient multi-carrier and frequency modulation schemes [2], transceiver design [11], pre-and post-equalization [12], [13], and channel capacity for dimmable VLC [14]. In the outdoor environments, as part of the 5G wireless networks, VLC can also play a significant role in a number of applications including intelligent transport systems (ITSs), the street-level access networks, Internet of things, etc. In [15], the concept of automotive lighting

in ITSs, was introduced by combining VLC and visible light positioning. A VLC-based simulation model for automotive applications was proposed in [16], where simulated channel models reflecting practical conditions for the usage of VLC in ITSs were provided. An environmental-adaptive receiver (Rx) to maximize the communication efficiency for automotive applications was proposed, in [17]. A new non-stationary regular-shaped geometry-based stochastic model (RS-GBSM) for vehicular VLC channels was proposed in [18]. In [19], a comprehensive channel modeling was carried out to quantify the effect of rain and fog on a vehicle-to-vehicle (V2V)-VLC link. In [20], the authors analyzed different precoding and equalization schemes for a 2×2 MIMO-based V2V-VLC system. Note that, precoding is a technique that exploits transmission diversity by weighting the information stream. A 3-D massive MIMO-based channel model for V2V communications was proposed in [21]. Contrary to the conventional MIMO channel model that characterizes the plane wavefront assumption, the authors assumed a spherical wavefront [21]. Recently, a V2V-VLC simulation-based channel modeling was reported in [22]. Moreover, different path loss expressions were proposed, and their comparative study is investigated [22]. In [23], a novel technique was introduced to increase the transmission linkspan of a rolling shutter-based optical camera communications (OCC) system to 400 m by reducing the spatial bandwidth of the camera in the out-of-focus regions. A V2V communications system employing OCC was studied in [24]. It was reported in [24] that, the system data rates are entirely dependent on the camera frame rate and the symbol duration. A prediction-based channel gain model and a multi-hop relay-based routing algorithm were proposed for V2V-VLC networks, in [25]. In [26], a low-complexity least-squares-based post-distortion algorithm was proposed for a multi-hop, V2V-VLC link. The formulated algorithm mitigates the V2V-VLC channel impairments by using a low dimensional approximation of the random Fourier features. Recently, a geometry-based stochastic channel model for V2V communications was proposed in [27]. The authors considered an urban environment and then parametrized the model from measurements [27].

B. Research Gap, Motivation, and Problem Statement

The study in [22] (a simulation-based channel modeling) considered a simplistic single-lane road-based V2V-VLC scenario. Moreover, the authors in [22] did not take into account the presence of other parked or mobile vehicles in the vicinity. Therefore, in [22], the lateral shift of vehicles and longitudinal separation between two communicating vehicles was considered to be deterministic.

Note that, due to parked or mobile vehicles in the vicinity of two communicating vehicles, the lateral shift of vehicles needs to be considered in a practical V2V-VLC system. Further, since LED-based VLC is mainly intended for short-distance communications, the longitudinal separation between two communicating vehicles will affect the system performance significantly. Furthermore, in outdoor environments, the effect of atmospheric turbulence (AT) of a practical V2V-VLC scenario has not been taken into account in [22]. Note that, AT induces fluctuations in the transmitted optical beam, which degrades the communication link performance significantly [28]. To this end, in this research, a more practical V2V-VLC model in a two-lane road and considering the effect of AT and other realistic system parameters (as tabulated in Table I) under the random lateral shift and the longitudinal separation is proposed and analyzed. We consider two realistic scenarios *(i)* **scenario 1 with the random lateral shift of vehicles and deterministic longitudinal separation between two vehicles; and** *(ii)* **scenario 2 with the longitudinal separation between two vehicles and the lateral shift of vehicles are considered to be random and deterministic, respectively.**

The work in [29] utilized the well-established infrastructure-to-vehicle (I2V) model and demonstrated the simulation results only. In [30], the authors analyzed the performance of a cooperative (relaying-based) full-duplex V2V-VLC system. In [31–34], an experimental investigation of the V2V-VLC system is reported. All these works did not emphasize the **comprehensive modeling** of a V2V-VLC system. **To be more specific, all the practical characteristics of a dynamic V2V-VLC environment were not modeled and envisioned in these works, such as *random path loss* due to the *random mobility* of the vehicle, *random lateral shift* of the vehicle, *random longitudinal separation* of the vehicle, modeling of the joint impact of path loss and atmospheric turbulence (AT) etc.** To this end, let us **outline** the **importance** of comprehensive modeling of the considered V2V-VLC system with the help of the following supporting statements:

- In a **dynamic/practical** V2V-VLC scenario, vehicles change positions with respect to (w.r.t.) their speed, the road layout, and other nearby parked/ mobile vehicles. This dynamic environment has a significant impact on the V2V-VLC link performance, because of the short transmission range in VLC. Therefore, considering the **practical characteristics** such as **random mobility**, **random path loss**, **random lateral shift** and **random longitudinal separation** is important to ensure accurate system modelling as part of intelligent transportation systems.

Table I
NOTATIONS USED IN THIS PAPER

W_L	Width of single lane
W_v	Width of vehicle
d	Longitudinal separation between the two vehicles
d_h	Lateral shift of the vehicle
ϕ_1 and ϕ_2	Angles of irradiance w.r.t Tx1 and Tx2
$\theta_1$and θ_2	Angles of incidence w.r.t Tx1 and Tx2
L_i	Propagation distance from the i^{th} transmitter (Tx)
Ψ	Field-of-view (FOV) angle of the receiver (Rx)
D_R	Aperture diameter of the Rx

- Further, to envision the impact of the outdoor environment on the considered V2V-VLC system, modeling the **joint impact** of path loss and AT conditions is **crucial**.

In light of the above background, we observe that most of the literature on V2V-VLC emphasized the channel modeling part and was not focused on the comprehensive modeling of the V2V-VLC system and performance analysis of the same. ***Motivated by this, in this work, we specifically emphasize the comprehensive modeling of a V2V-VLC system under practical considerations which have not been taken into account in the literature so far.*** To this end, in the subsequent subsection, we summarize the key contributions of our work.

C. Key Contributions

Motivated by the aforementioned background, the key contributions depicting the significance of this research are highlighted as follows:

- A two-lane road-based V2V-VLC model under two different scenarios (as highlighted in Subsection I. B) is considered. Since weather conditions have a significant impact on the V2V-VLC performance, we also analyze the impact of different weather conditions on the considered model.
- Because of the dynamic V2V environment, we **model** the lateral movement and the longitudinal separation of the vehicle as **random** with a specific probability distribution function (PDF). **Therefore, differing from the existing literature wherein deterministic lateral shift and**

longitudinal separation are considered, in this work, a more realistic and generalized approach is adopted to take into account the lateral shift and longitudinal separation of the vehicle.

- Further, differing from the existing literature, a **novel channel model** is taken into account that considers the **joint impact** of path loss and AT. Note that path loss has a significant impact on the V2V-VLC system.
- Since V2V-VLC is highly dependent on the line-of-sight (LOS) communication, we also model the road surface reflections and the LOS blocking with an **associated path loss** and analyze their impact on the proposed model.
- Furthermore, the performance of the proposed V2V-VLC model is investigated under the considered scenarios with different performance metrics such as path loss, outage probability, average bit error rate (ABER), and diversity property. Novel analytical expressions for path loss, outage probability, and ABER are derived. Based on the derived ABER expressions corresponding to the two V2V-VLC scenarios, this work, for the first time, investigates the **diversity property** of the V2V-VLC system.

D. Related Work and Comparison

In this subsection, we compare our proposed work with the existing literature and summarize the new **insights** as follows:

- In [29], the authors analyzed the performance of the V2V-VLC system under different *weather conditions* by considering a Lambertian emission-based LOS channel model, which is only valid for indoor VLC scenarios [2], [4]. Such a channel model is not valid for a dynamic outdoor V2V-VLC system wherein the path loss will have a significant impact on the system performance [22]. Therefore, the findings of the authors in [29] under different weather conditions are inaccurate. **To this end, in this work, for the first time, a realistic channel model that takes into account the complete outdoor V2V-VLC path loss with AT under different weather conditions is proposed.**
- In [30], the authors analyzed the performance of a cooperative full-duplex V2V-VLC system. In [31–34], an experimental investigation of the V2V-VLC system is reported. **However, all these**

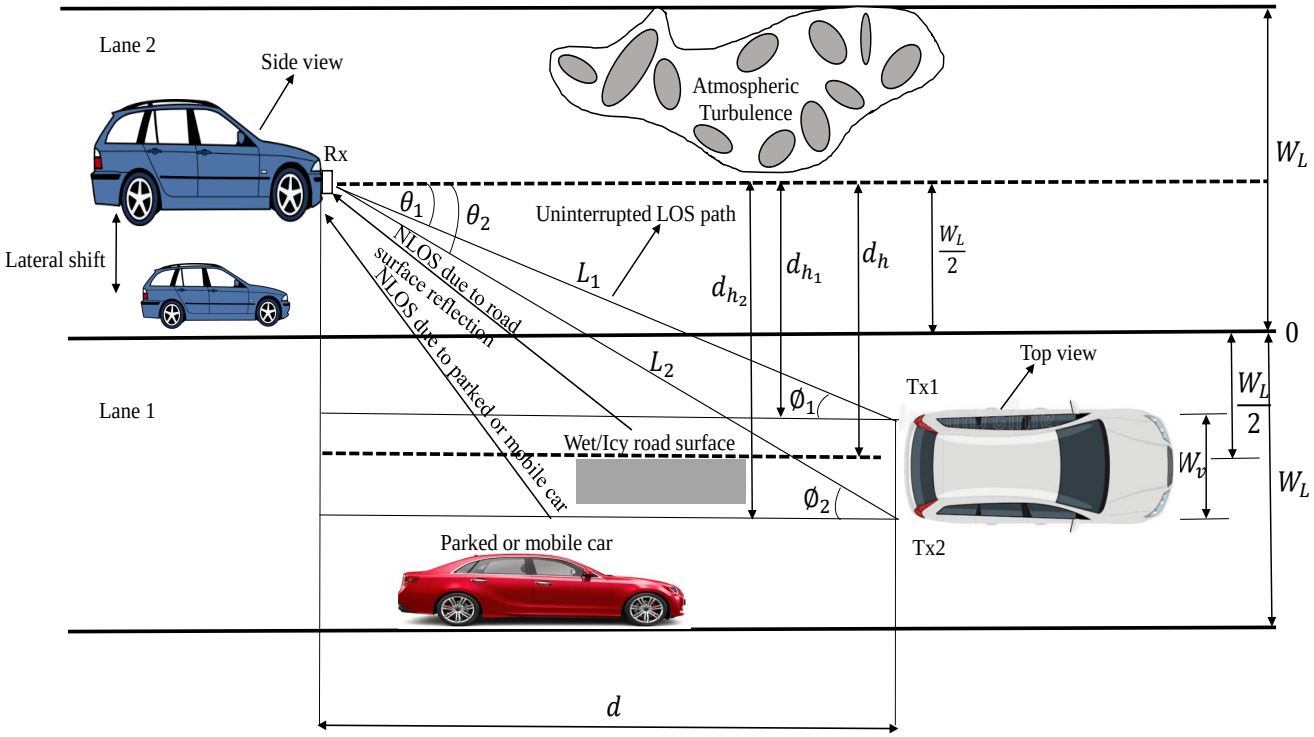

Figure 1. Proposed two-lane road-based V2V-VLC model.

works considered the lateral shift of the vehicle to be deterministic, which is impractical. To this end, in this work, for the first time, we **model** the lateral movement of the vehicle as random with a uniform PDF and analyze its impact on the different performance metrics. **Therefore, we emphasize a realistic and generalized approach to take into account the lateral movement of the vehicle.**

- In [34], an experimental investigation of an infrastructure-to-vehicle-to-vehicle (I2V2V) VLC system for ITSs is done. However, the authors considered the longitudinal (inter-vehicle) distance to be deterministic, which is impractical due to the random mobility of the vehicle. **To this end, in this work, we model the longitudinal/inter-separation of the vehicle as random with an inverse-gaussian PDF.**

To be more specific, the mobility of the vehicle, has not been considered *random* in the existing literature, which is unrealistic. Further, apart from the above-mentioned differences, the **major** difference is the modeling of all the practical characteristics of V2V-VLC and their impact on the proposed model (as discussed in Subsection I. C), which have not been taken into account in all these works.

II. PRELIMINARIES

In this section, we present and discuss the considered V2V-VLC system and channel models. The proposed V2V-VLC model is discussed with detailed insights.

A. System Parameters Description and Derived Geometric Relations

A two-lane road-based V2V-VLC system is considered, as shown in Fig. 1. It can be seen from Fig. 1 that, the two communicating vehicles are in lanes 1 and 2. The backlights of the leading vehicle are used as the Txs and a photodetector-based Rx is deployed at the bumper of the following vehicle in lane 2. In Table I, all the system parameters are tabulated. The values corresponding to the system parameters depicted in Table I will be provided in Section V. Note that, according to the geometry depicted in Fig. 1, $\phi_1 = \theta_1$ and $\phi_2 = \theta_2$. The lateral shift corresponding to the i^{th} Tx is defined as $d_{h_i} \triangleq d_h \pm \frac{W_v}{2},\ i = 1, 2$. Moreover, the LOS propagation distance (as depicted in Fig. 1) for the i^{th} angle is defined as $L_i \triangleq \sqrt{d^2 + d_{h_i}^2}$. Since L_i is dependent on d_{h_i}, and therefore, the incidence angle and its dependence on d_{h_i} can be expressed as:

$$\theta_i = \cos^{-1}\left(\frac{d}{L_i}\right). \tag{1}$$

From the proposed V2V-VLC model shown in Fig. 1, it is noted that, d_h varies between 0 and ($2W_L$-W_v). In other words, d_h is random and it can take values between 0 and ($2W_L$-W_v). Mathematically, it can be expressed as follows[1]:

$$0 \leq d_h \leq (2W_L - W_v). \tag{2}$$

Relation between d, L_i, and FOV (Ψ): For the Rx to detect LOS signals, the following condition must be satisfied:

$$\begin{aligned} &0 \leq \theta_i \leq \Psi, \\ &\Rightarrow \cos(\theta_i) \geq \cos(\Psi), \\ &\therefore \boxed{L_i \leq \frac{d}{\cos(\Psi)}.} \end{aligned} \tag{3}$$

Substituting L_i in (3), we obtain:

[1] d_h is assumed to be random within a range for a given lane and vehicle width as depicted in Eq. (2). Moreover, due to the mobility of other vehicles in the vicinity, d_h varies slowly over a small duration of time T within the specified range.

$$d_{h_i}^2 \leq d^2\Big(\frac{1-\cos^2(\Psi)}{\cos^2(\Psi)}\Big),$$
$$\therefore \boxed{d_{h_i} \leq d\ \tan(\Psi).} \tag{4}$$

Moreover, we have the following relation:

$$d_{h_i} = d_h \pm \frac{W_v}{2}. \tag{5}$$

Therefore, from (4) and (5), we get:

$$\Big(d_h \pm \frac{W_v}{2}\Big) \leq d\ \tan(\Psi). \tag{6}$$

Based on (6), we have the following implications:

- For d_{h_1}:

$$d_h - \frac{W_v}{2} \leq d\ \tan(\Psi),$$
$$\Rightarrow d_h \leq d\ \tan(\Psi) + \frac{W_v}{2}. \tag{7}$$

Note that if the condition in (7) is satisfied, then the LOS signal, L_1, is detected by the Rx.

- For d_{h_2}:

$$d_h + \frac{W_v}{2} \leq d\ \tan(\Psi),$$
$$\Rightarrow d_h \leq d\ \tan(\Psi) - \frac{W_v}{2}. \tag{8}$$

Note that if the condition in (8) is satisfied, then the LOS signal, L_2, is detected by the Rx. Therefore, taking into account (7) and (8), we can have the following implication:

$$\boxed{d_h \leq d\ \tan(\Psi) \pm \frac{W_v}{2}.} \tag{9}$$

Remark 1: Note that a practical V2V-VLC environment is dynamic because of the vehicles changing positions w.r.t. the road and other vehicles. Therefore, based on the derived Eq. (9), we infer that under the impact of the lateral shift, i.e., d_h, the Rx will detect L_1 and L_2 with a constraint given in (9). Moreover, contrary to (2), the randomness in d_h is jointly restricted by the three different system parameters as depicted in (9).

Due to the dynamic nature of the V2V-VLC environment, a narrow FOV-based Rx might be problematic in such mobile conditions. Therefore, we consider a wide FOV-based Rx to maximize

the reception angle.

B. Channel Model

For the proposed V2V-VLC model, the received signal by the vehicle in lane 2 is given by:

$$\mathbf{y} = \eta \mathbf{h} \mathrm{x} + \mathbf{e}, \tag{10}$$

where $\mathbf{y} = [y_1, y_2]^T \in \mathbb{R}^{2\times 1}$ is the received signal vector, η is the photodetector's responsivity, $\mathrm{x} \geq 0$ denotes the non-negative visible-light signal from the two Txs, and $\mathbf{e} = [e_1, e_2]^T$ denotes the noise vector. Moreover, $\mathbf{h} = [h_1, h_2]^T \in \mathbb{R}^{2\times 1}$ is the channel coefficient vector, and each element in $\mathbf{h}$ can be modeled as:

$$h_i = h_{a_i} (h_i^{PL})^{avg}, \tag{11}$$

where h_{a_i} expresses the AT, which signifies the impact of environmental conditions, and $(h_i^{PL})^{avg}$ denotes the average path loss. Since VLC is a short-distance communication, without loss of generality, the PDF of h_{a_i} can be modeled as a lognormal distribution [13]:

$$f_{h_{a_i}}(h_{a_i}) = \frac{\exp\left(- \frac{\left(\ln(h_{a_i}) + 2\sigma_L^2 \right)^2}{8\sigma_L^2} \right)}{2h_{a_i}\sqrt{2\pi\sigma_L^2}}, \quad h_{a_i} > 0, \tag{12}$$

where σ_L^2 is the log-amplitude variance.

Remark 2: Considering a practical outdoor V2V-VLC scenario, in this work, we investigate the performance and diversity property of the proposed V2V-VLC model under the combined impact of path loss and AT as depicted in (11).

Further, a maximum-likelihood (ML) Rx for the proposed V2V-VLC model is expressed as:

$$\widehat{\mathrm{x}} = \min_{\mathrm{x}\in\{0,1\}} \left| \mathbf{y} - \eta \mathbf{h} \mathrm{x} \right|^2, \tag{13}$$

where x denotes an on-off keying (OOK) symbol, and $\widehat{\mathrm{x}}$ denotes the detected symbol at the Rx. It is assumed that the channel state information (CSI) is known at the Rx. With this, d_h can be estimated to some extent in the small time slots within the range, i.e., $0 \leq d_h \leq (2W_L - W_v)$.

III. Performance Metrics for the Proposed V2V-VLC Model Corresponding To Scenario 1

In this section, we will investigate the performance of the proposed V2V-VLC model corresponding to the scenario 1. Since VLC using LED lights is mostly intended for a short-distance communications, the lateral shift of the vehicle has a significant impact on the V2V-VLC system performance. Further, to investigate the performance of the proposed V2V-VLC model, we consider different performance metrics such as the path loss, outage probability, ABER, and diversity.

Scenario 1*: Here, the random lateral shift of the vehicle and the deterministic longitudinal separation between the two communicating vehicles is considered.*

A. Investigation of Average Path Loss

We build upon the path loss expression given in [22, Eq.(7)]. However, unlike [22], wherein the lateral shift of the vehicle is considered to be deterministic, in this work, the lateral shift of the vehicle is quantified as random. Therefore, contrary to [22], a more practical path loss expression is derived in this paper. The path loss for one of the two LOS propagation paths (as depicted in Fig. 1) is given by:

$$h_1^{PL} = \frac{1}{2}\Big(\frac{D_R}{\xi}\Big)^2 \frac{(\cos(\theta_1))^{2/\epsilon}}{L_1^2}\exp(-cL_1). \tag{14}$$

Note that, ξ and ϵ are the correction coefficients corresponding to different weather conditions, and c is the extinction coefficient. The values of ξ, ϵ and c are tabulated in [22] for different weather conditions. Since $\cos(\theta_1) = \frac{d}{L_1}$, we can express (14) as:

$$h_1^{PL} = \frac{1}{2}\Big(\frac{D_R}{\xi}\Big)^2 \frac{d^{2/\epsilon}}{L_1^{2+2/\epsilon}}\exp(-cL_1). \tag{15}$$

Now, let us consider that d_{h_1} is uniformly distributed, i.e., $d_{h_1} \sim \mathcal{U}\left(\frac{-W_V}{2}, 2W_L - \frac{W_V}{2}\right)$. Accordingly, $L_1 \sim \mathcal{U}\left(a = \sqrt{d^2 + \frac{W_V^2}{4}}, b = \sqrt{d^2 + \left(2W_L - \frac{W_V}{2}\right)^2}\right)$. Therefore, the average path loss is given by:

$$(h_1^{PL})^{avg} = \int_0^\infty h_1^{PL} f_{L_1}(L_1) dL_1, \tag{16}$$

where

$$f_{L_1}(L_1) \triangleq \begin{cases} \frac{1}{b-a}, & a \leq L_1 \leq b \\ 0, \text{elsewhere} \end{cases} \tag{17}$$

Remark 3: It can be observed from (15) that the path loss depends on L_1. Moreover, L_1 is dependent on d_{h_1} (as per the geometric relation given in Subsection II. A). Further, since d_{h_1} is uniformly distributed, therefore, the path loss depends on the uniformly distributed lateral shift of the vehicle. Employing (15) and (17) into (16), we get:

$$(h_1^{PL})^{avg} = \frac{1}{2}\Big(\frac{D_R}{\xi}\Big)^2 \frac{d^{2/\epsilon}}{b-a} \int_a^b \exp(-cL_1) \frac{1}{L_1^{2+2/\epsilon}} dL_1. \tag{18}$$

Let $k = 2 + \frac{2}{\epsilon}$ and $cL_1 = x$, a closed-form expression corresponding to (18) is obtained as:

$$(h_1^{PL})^{avg} = \frac{D_R^2 d^{2/\epsilon} c^{k-1}}{2\xi^2(b-a)} \Big[\Gamma(1-k, ac) - \Gamma(1-k, bc)\Big], \tag{19}$$

where $\Gamma(\cdot, \cdot)$ is the upper incomplete-gamma function [35]. Similarly, a closed-form expression for the other LOS propagation path can be obtained. Thus, the effective path loss at the Rx corresponding to scenario 1 is given by:

$$h_{\text{Eff}}^{PL} = 10\log_{10}\Big(\sum_{i=1}^{2} (h_i^{PL})^{avg}\Big). \tag{20}$$

B. Investigation of Outage Probability

In this subsection, we investigate the outage performance of the proposed V2V-VLC model corresponding to scenario 1. Since LED-based VLC is mainly intended for short-distance communications, therefore, the investigation of outage performance is of significant interest. An outage of a communication system is a probabilistic scenario wherein the signal-to-noise ratio (SNR) corresponding to all the communication links falls below certain threshold SNR. Taking (11) and (12) into account, the PDF of h_i is obtained as:

$$f_{h_i}(h_i) = \frac{\exp\left(-\frac{\left(\ln\left(\frac{h_i}{(h_i^{PL})^{avg}}\right) + 2\sigma_L^2\right)^2}{8\sigma_L^2}\right)}{2h_i\sqrt{2\pi\sigma_L^2}}, \quad h_i > 0. \tag{21}$$

Therefore, the average received electrical SNR is given by:

$$\gamma_i = \frac{(\eta P_t h_i)^2}{\sigma_i^2} = R_i h_i^2, \tag{22}$$

where $R_i = \frac{(\eta P_t)^2}{\sigma_i^2}$, P_t is the transmit optical power corresponding to each Tx, and σ_i^2 denotes the variance of noise e_i.

Remark 4: For the outdoor VLC, the ambient-induced shot noise is the dominant noise. To be more specific, let us denote the shot noise by $\sigma_{i,\text{Shot}}^2$, which is given by $\sigma_i^2 = \sigma_{i,\text{Shot}}^2 = 2q\eta B P_R + 2qBI_2 I_{\text{bg}}$. Note that $P_R = P_t h_i$. Further, all the parameters are defined in [36]. Note that $\sigma_{i,\text{Shot}}^2$ can be modeled as Gaussian noise [36].

Further, the selective transmission scheme is applied by using the criterion of maximizing the output SNR as defined by:

$$\gamma \triangleq \max(\gamma_1, \gamma_2). \tag{23}$$

Owing to the sufficient separation between the Tx1 and Tx2, we assume γ_1 is independent of γ_2. Therefore, the outage probability can be expressed as:

$$P_{out} = \prod_{i=1}^{2} \int_0^{\sqrt{\frac{\gamma_{th}}{R_i}}} f_{h_i}(h_i) dh_i. \tag{24}$$

In (24), γ_{th} denotes the threshold SNR. On substituting (21) into (24), we get:

$$P_{out} = \prod_{i=1}^{2} \int_0^{\sqrt{\frac{\gamma_{th}}{R_i}}} \frac{\exp\left(- \frac{\left(\ln\left(\frac{h_i}{(h_i^{PL})^{avg}}\right) + 2\sigma_L^2 \right)^2}{8\sigma_L^2} \right)}{2h_i\sqrt{2\pi\sigma_L^2}} dh_i. \tag{25}$$

Applying change of variables method, i.e., $t_i = \frac{\left(\ln\left(\frac{h_i}{(h_i^{PL})^{avg}}\right) + 2\sigma_L^2 \right)}{2\sigma_L}$, a closed-form corresponding to (25) is obtained as:

$$P_{out} = \prod_{i=1}^{2} Q\left(- \frac{\ln\left(\frac{\sqrt{\gamma_{th}}\sigma_i}{(h_i^{PL})^{avg}\eta P_t}\right) + 2\sigma_L^2}{2\sigma_L} \right), \tag{26}$$

where $Q(.)$ is Gaussian q-function.

Remark 5: Let $m_i = \left(- \frac{\ln\left(\frac{\sqrt{\gamma_{th}}\sigma_i}{(h_i^{PL})^{avg}\eta P_t}\right) + 2\sigma_L^2}{2\sigma_L} \right)$ and thus $P_{out} = \prod_{i=1}^{2} Q(m_i)$. Note that m_i is a monotonously decreasing function with respect to σ_i. Moreover, P_{out} is a monotonously decreasing function with respect to m_i. Therefore, P_{out} is a monotonously decreasing function with respect to

σ_i, which indicates that the larger the variance of the noise is, the worse the system performance becomes.

C. Investigation of ABER

The ABER corresponding to the proposed V2V-VLC model for scenario 1 can be expressed as:

$$\text{ABER} = \int_0^\infty \int_0^\infty Q\Big(\sqrt{\gamma_i(h_1+h_2)^2}\Big) \times f_{h_1}(h_1) f_{h_2}(h_2) dh_1 dh_2. \tag{27}$$

To determine a closed-form expression of (27), let us consider the inner integral of (27):

$$I_1 = \int_0^\infty Q\Big(\sqrt{\gamma_i(h_1+h_2)^2}\Big) f_{h_1}(h_1) dh_1. \tag{28}$$

Employing the relation $Q(x) = \frac{1}{2}\text{erfc}(\frac{x}{\sqrt{2}})$ in (28), and substituting (21), for $i = 1$, into (28), we get:

$$I_1 = \int_0^\infty \frac{1}{2}\text{erfc}\Big((h_1+h_2)\sqrt{\frac{\gamma_i}{2}}\Big) \times \frac{\exp\left(-\frac{\left(\ln\left(\frac{h_1}{(h_1^{PL})^{avg}}\right)+2\sigma_L^2\right)^2}{8\sigma_L^2}\right)}{2h_1\sqrt{2\pi\sigma_L^2}} dh_1. \tag{29}$$

Applying change of variables method, i.e., $t = \frac{\left(\ln\left(\frac{h_1}{(h_1^{PL})^{avg}}\right)+2\sigma_L^2\right)}{2\sigma_L}$, (29) can be expressed as:

$$I_1 = \frac{1}{2\sqrt{2\pi}} \int_0^\infty \text{erfc}(ae^{bt}+d) e^{-\frac{t^2}{2}} dt, \tag{30}$$

where $a = (h_1^{PL})^{avg} e^{-2\sigma_L^2}\sqrt{\frac{\gamma_i}{2}}$, $b = 2\sigma_L$, and $d = h_2\sqrt{\frac{\gamma_i}{2}}$. Again applying the change of variables method, i.e., $z = e^{bt}$ to (30), we get:

$$I_1 = \frac{1}{2\sqrt{2\pi}} \int_1^\infty \frac{1}{bz}\text{erfc}\Big(a\big(z+\frac{d}{a}\big)\Big) e^{-\frac{lnz}{b^2}} dz. \tag{31}$$

A closed-form expression corresponding to (31) can be evaluated using MATHEMATICA software as given by:

$$I_1 = \frac{b}{2\sqrt{2\pi}}\left(\text{erfc}(d) - \frac{d\text{ExpIntegralE}[\frac{1}{2}(1+\frac{1}{b^2}), d^2]}{\sqrt{\pi}}\right), \tag{32}$$

where $\mathrm{ExpIntegralE}[n, z]$ gives the exponential integral function $E_n(z)$ [37]. Therefore, (27) reduces to:

$$\begin{aligned}\mathrm{ABER} &= \int_0^\infty I_1 f_{h_2}(h_2) dh_2 \\ &= \int_0^\infty I_1 \frac{\exp\left(- \frac{\left(\ln\left(\frac{h_2}{(h_2^{PL})^{avg}} \right) + 2\sigma_L^2 \right)^2}{8\sigma_L^2} \right)}{2h_2\sqrt{2\pi\sigma_L^2}} dh_2. \end{aligned} \tag{33}$$

Applying change of the variables method, i.e., $u = \frac{\left(\ln\left(\frac{h_2}{(h_2^{PL})^{avg}} \right) + 2\sigma_L^2 \right)}{2\sigma_L}$, (33) can be expressed as:

$$\mathrm{ABER} = \int_0^\infty I_1 \frac{1}{\sqrt{2\pi}} e^{-\frac{u^2}{2}} du. \tag{34}$$

On substituting (32) into (34), we get:

$$\mathrm{ABER} = \frac{b}{4\pi} \times \int_0^\infty \left(\mathrm{erfc}(d) - \frac{d\mathrm{ExpIntegralE}[\frac{1}{2}(1 + \frac{1}{b^2}), d^2]}{\sqrt{\pi}} \right) e^{-\frac{u^2}{2}} du. \tag{35}$$

Now, to evaluate (35), let us have the following two considerations:

$$I_2 = \int_0^\infty \mathrm{erfc}(d) e^{-\frac{u^2}{2}} du. \tag{36}$$

and

$$I_3 = \int_0^\infty \frac{d\ \mathrm{ExpIntegralE}[\frac{1}{2}(1 + \frac{1}{b^2}), d^2]}{\sqrt{\pi}} e^{-\frac{u^2}{2}} du. \tag{37}$$

To compute I_2, applying the change of variables method, i.e., $t = \frac{\left(\ln\left(\frac{h_2}{(h_2^{PL})^{avg}} \right) + 2\sigma_L^2 \right)}{2\sigma_L}$, we get:

$$I_2 = \int_0^\infty \mathrm{erfc}(ge^{bt}) e^{-\frac{t^2}{2}} dt, \tag{38}$$

where $g = (h_2^{PL})^{avg} e^{-2\sigma_L^2} \sqrt{\frac{\gamma_i}{2}}$. Employing a transformation of $z = e^{bt}$, a closed-form solution corresponding to (38) is obtained as:

$$I_2 = b\Big[\mathrm{erfc}(g) - \frac{g\mathrm{ExpIntegralE}[\frac{1}{2}(1 + \frac{1}{b^2}), g^2]}{\sqrt{\pi}} \Big]. \tag{39}$$

Adopting the similar technique for obtaining the closed-form of I_2, a closed-form corresponding to I_3 is obtained as follows:

$$I_3 = gbe^{-g^2} \times \frac{\left(2b^2 - \left(1 + (-1 + 2g^2)\right)b^2 e^{g^2} \text{ExpIntegralE}[\frac{1}{2}(-1 + \frac{1}{b^2}), g^2]\right)}{2(-1 + b^2)\sqrt{\pi}}. \tag{40}$$

Now, taking (35), (36) and (37) into account, ABER can be expressed as:

$$\therefore \text{ABER} = \text{abs}(\frac{b}{4\pi}(I_2 - I_3)), \tag{41}$$

where the closed-form expressions corresponding to I_2 and I_3 are given by (39) and (40), respectively. Further, $\text{abs}(.)$ denotes the absolute value. Since $I_2 < I_3$, therefore, the absolute value of ABER is considered in (41).

D. Investigation of Diversity Order

Before we begin with the investigation of the diversity property for the considered V2V-VLC system, let us motivate our finding by discussing the existing works on diversity order.

- For instance, in [38], the diversity performance corresponding to the single-input single-output (SISO) free-space optical (FSO) system and MIMO-FSO system under Gamma-Gamma fading is analyzed. It is observed that the diversity gain of the SISO-FSO system only depends on the minimum of α and β, where α and β characterize a specific turbulence regime. As far as the MIMO-FSO configuration is considered, it is concluded from Eq. (26) that employing repetition coding across transmit lasers and equal gain combining at the Rx can exploit full diversity gain.
- In [39], the diversity performance of a MIMO-FSO system assuming repetition coding across lasers with a multipulse pulse-position-modulation (PPM) scheme is analyzed. It is shown by the analysis that full transmit and receiver diversity can be attained without special coding.
- Finally, in [40], it is shown through power allocation that the cooperative diversity and BER performance of the considered system can be significantly optimized.

However, in this work, we focus on a V2V-VLC scenario and the associated system parameters, which have a significant impact on the V2V-VLC performance. Most importantly, differing from the

above works, a novel channel model that takes into account the **joint impact** of path loss and AT is considered. **Further, in a V2V-VLC system, the diversity performance investigation is highly dependent on the weather conditions.** Therefore, the investigation of the diversity performance corresponding to such a system is a significant metric of interest. The diversity corresponds to the slope of decay of ABER versus the SNR plot at asymptotically high values of SNR. Mathematically, at very high SNR, ABER can be expressed as:

$$\mathrm{ABER}_{\gamma_\mathrm{i}\to\infty} \propto \gamma_i^{-d_o}, \tag{42}$$

where d_o denotes the diversity order. Therefore, taking (42) into account, let us first determine d_o corresponding to the closed-form expression of I_2 given in (39), at a very high value of SNR. With (42), we will consider only the terms proportional to the exponent of γ_i and the constants or other factors multiplied with γ_i can be ignored as they do not have any significance in finding d_o. Now, in (39), at a very high value of SNR, $\mathrm{erfc}(g) = 0$. Further, note that $E_n(z) = \int_1^\infty \frac{e^{-zt}}{t^n} dt = \int_1^\infty \frac{e^{-g^2 t}}{t^{\frac{1}{2}(1+\frac{1}{b^2})}} dt$. Therefore, employing Taylor series expansion of an exponential function corresponding to $E_n(z)$, i.e., e^{-g^2}. Further, representing the series in a form given in (43) to determine the dominant term at a very high SNR as follows:

$$\begin{aligned} e^{-g^2} &= 1 - \gamma_i + \gamma_i^2 - \gamma_i^3 + \cdots\cdots, \\ &= \gamma_i^3 \Big(\frac{1}{\gamma_i^3} - \frac{1}{\gamma_i^2} + \frac{1}{\gamma_i} - 1 + \cdots\cdots \Big). \end{aligned} \tag{43}$$

At a very high SNR, considering the dominant terms in (43), we have $e^{-g^2} = \gamma_i^2$. Therefore, we obtain:

$$I_2 \propto \gamma_i^2. \tag{44}$$

Similarly, the exponent of γ_i corresponding to (40) is obtained as:

$$I_3 \propto \gamma_i^3. \tag{45}$$

Now, $I_2 - I_3 \propto (\gamma_i^2 + (-\gamma_i^3))$. Therefore, the ABER at very high SNR will be:

$$\mathrm{ABER}^{\mathrm{Scenario1}}_{\gamma_\mathrm{i}\to\infty} \propto \gamma_i^2. \tag{46}$$

Thus the diversity order corresponding to scenario 1 is obtained as $d_o = 2$.

Remark 6: We employ a repetition coding (RC) scheme for the data transmission for which the same symbol is transmitted from both the Txs. Note that the RC scheme is able to provide full diversity.

IV. Performance Metrics for the Proposed V2V-VLC Model Corresponding To Scenario 2

In this section, we investigate the performance of the proposed V2V-VLC model corresponding to scenario 2. Due to the short-distance nature of VLC, the longitudinal separation between the two communicating vehicles has a significant impact on the V2V-VLC system performance. To derive the performance metrics of scenario 2, we build upon the analytical framework of scenario 1.

Scenario 2*: A more practical scenario in which the longitudinal separation between the two communicating vehicles is quantified as random. Contrary to scenario 1, the presence of parked or mobile vehicles in the vicinity of two communicating vehicles is also taken into account, as depicted in Fig. 1. Therefore, the non-line-of-sight (NLOS) signal components arising due to parked/mobile vehicles and from the road surface reflection are also considered.*

Let Z be the event corresponding to the LOS blockage whose probability mass function (PMF) can be modeled by Bernoulli distribution:

$$\Pr[Z=z]=\begin{cases} p, z=1 \\ 1-p, z=0, \end{cases} \tag{47}$$

where $\Pr[.]$ denotes the probability.

Remark 7: The event $z=1$ (direct-path obstruction between the Tx and Rx) corresponds to an event of blocked LOS with probability p. However, when $z=0$ (no direct-path obstruction between the Tx and Rx), the complete VLC channel comprises both the LOS and NLOS signal components. Note that, the NLOS signal components arise from obstructions in the vicinity of two communicating vehicles, such as parked /mobile vehicles or reflections from the road surface.

Remark 8: There are some works in the literature of indoor VLC, which consider blockage such as, [2]. Note that in an indoor VLC scenario, the blockage is mainly because of the **opaque objects.** However, in this work, we specifically emphasize the modeling of the LOS blockage with an **associated path loss** (as depicted in Eq. (48)) for an outdoor V2V-VLC system, which is **highly**

dependent on the weather conditions. Moreover, because of the short-distance nature of VLC, this blockage has a significant impact on the V2V-VLC system performance. Further, in this work, the novel channel model that considers the **joint impact** of path loss and AT is completely different from an indoor VLC channel. **Therefore, this work emphasizes blockage under a completely different communication environment.**

A. Investigation of Average Path Loss

The total path loss at the Rx corresponding to LOS as well as NLOS signal components can be expressed as:

$$\begin{aligned} h^{PL}_{\text{Total}-\text{Rx}} &= \sum_{\beta=0}^{n_d} h^{PL}(\beta) = h^{PL}(0) + \sum_{\beta=1}^{n_d} h^{PL}(\beta) \\ &= p\Big(n_d h^{PL}(\beta)\Big) + (1-p)\Big((n_d+1)h^{PL}(0)\Big), \end{aligned} \tag{48}$$

where $h^{PL}(0)$ and $\sum_{\beta=1}^{n_d} h^{PL}(\beta)$ are the path loss corresponding to LOS and NLOS, respectively, with n_d being the number of diffused signal components.[2] Now, the path loss corresponding to the i^{th} LOS propagation path is given by:

$$h^{PL}_i(d) = p\left(\frac{1}{2}\Big(\frac{D_R}{\xi}\Big)^2 \frac{d^{2/\epsilon}}{L_i^{2+2/\epsilon}}\exp(-cL_i)\right) + (1-p)\left(\frac{1}{2}\Big(\frac{D_R}{\xi}\Big)^2 \frac{d^{2/\epsilon}}{L_i^{2+2/\epsilon}}\exp(-cL_i)\right). \tag{49}$$

The path loss presented in Eq. (49) considers both the LOS and NLOS depending upon the LOS blocking probability p. Considering that the two vehicles are sufficiently apart from each other, we assume the PDF of d to be inverse Gaussian distribution [41]. Considering a realistic V2V-VLC scenario, let us consider d to be random within a range of 0 to 50 m. For the considered range, the PDF of d can be written as:

$$f_d(d) = \frac{1}{0.989108} \times \sqrt{\frac{\lambda}{2\pi d^3}} \times \; e^{-\frac{\lambda(d-\mu)^2}{2\mu^2 d}}, 0 \leq d \leq 50. \tag{50}$$

Note that the area under the PDF for the PDF given in (50) is unity for the mean $\mu = 25$ and the shape parameter $\lambda = 0.01$.

[2]Because of the short-distance nature of VLC, the blockage of LOS is probabilistic (as depicted in Eq. (48)), i.e., there will not be many blockages. Therefore, it is assumed that the path loss corresponding to each diffused signal component is identical. However, we will consider non-identical diffused signal components in the future extension of this work.

Remark 9: Because of the short transmission distance of VLC, d is assumed to be random within a practical range of 0 - 50 m. Moreover, due to the mobility of other vehicles in the vicinity, d varies slowly over a small duration of time T within the specified range.

Therefore, the average path loss expression is given by:

$$(h_i^{PL})^{avg} = \int_0^{\infty} h_i^{PL}(d) f_d(d) dd. \tag{51}$$

On substituting (49) and (50) into (51), employing taylor series expansion of an exponential function, the average path loss can be expressed as:

$$\begin{aligned}(h_i^{PL})^{avg} = p\Bigg(&\frac{1}{0.989108} \times \frac{D_R^2\sqrt{\lambda}}{2\xi^2} \times \int_0^{50} \frac{1}{\sqrt{2\pi d^3}} \times \\ &\frac{d^{2/\epsilon}}{\left(\sqrt{d^2+d_{h_i}^2}\right)^{2+2/\epsilon}} \times \sum_{n=0}^{\infty}(-1)^n \frac{\left(c\sqrt{d^2+d_{h_i}^2}\right)^n}{n!} \times e^{-\frac{\lambda(d-\mu)^2}{2\mu^2 d}} dd\Bigg) \\ + (1-p)\Bigg(&\frac{1}{0.989108} \times \frac{D_R^2\sqrt{\lambda}}{2\xi^2} \times \int_0^{50} \frac{1}{\sqrt{2\pi d^3}} \times \\ &\frac{d^{2/\epsilon}}{\left(\sqrt{d^2+d_{h_i}^2}\right)^{2+2/\epsilon}} \times \sum_{n=0}^{\infty}(-1)^n \frac{\left(c\sqrt{d^2+d_{h_i}^2}\right)^n}{n!} \times e^{-\frac{\lambda(d-\mu)^2}{2\mu^2 d}} dd\Bigg).\end{aligned} \tag{52}$$

Therefore, using (48) the effective path loss at the Rx corresponding to scenario 2 will be:

$$h_{\text{Eff}}^{PL} = 10\log_{10}\left(\sum_{i=1}^{2} p\Big(n_d (h_i^{PL})^{avg}\Big) + (1-p)\Big((n_d+1)(h_i^{PL})^{avg}\Big)\right). \tag{53}$$

Note that the factor $(n_d + 1)$ in Eq. (53) represents the consideration of NLOS signal components with identical path loss.

Remark 10: The integral in (52) is a finite integral and can be swiftly evaluated using MATHEMATICA software. Therefore, further effort for simplifying (52) is not required.

B. Investigation of Outage Probability

In this subsection, we investigate the outage performance of the considered V2V-VLC model corresponding to scenario 2. Following the similar procedure of scenario 1, the closed-form expression corresponding to the outage probability of scenario 2 is given by:

$$P_{out} = \prod_{i=1}^{2} \int_{0}^{\frac{\ln\left(\frac{\sqrt{\frac{\gamma_{th}}{R_i}}}{(h_i^{PL})^{avg}}\right)+2\sigma_L^2}{2\sigma_L}} \Big[\frac{1}{\sqrt{2\pi}}\exp\big(-\frac{t_i^2}{2}\big)\Big] dt_i$$
$$= \prod_{i=1}^{2} Q\bigg(-\frac{\ln\Big(\frac{\sqrt{\gamma_{th}}\sigma_i}{(h_i^{PL})^{avg}\eta P_t}\Big)+2\sigma_L^2}{2\sigma_L}\bigg). \tag{54}$$

To consider the effective path loss at the Rx corresponding to LOS as well as NLOS signal components, the outage probability of the considered system will be:

$$P_{out} = \prod_{i=1}^{2} Q\bigg(-\frac{\ln\Big(\frac{\sqrt{\gamma_{th}}\sigma_i}{h_{i,\text{Eff}}^{PL}\eta P_t}\Big)+2\sigma_L^2}{2\sigma_L}\bigg), \tag{55}$$

where $h_{i,\text{Eff}}^{PL}$ is the effective path loss at the Rx corresponding to the i^{th} LOS link, and it can be obtained from (53).

Remark 11: Contrary to scenario 1, wherein the outage probability given in (26) depends on the longitudinal separation between the two communicating vehicles, the outage probability corresponding to scenario 2 given in (55) depends on lateral shift of the vehicle.

C. Investigation of ABER and Diversity Order

The PDF corresponding to the i^{th} propagation path incorporating the LOS as well as NLOS signal components for scenario 2 can be written as:

$$f_{h_i}(h_i) = \frac{\exp\left(-\frac{\left(\ln\left(\frac{h_i}{h_{i,\text{Eff}}^{PL}}\right)+2\sigma_L^2\right)^2}{8\sigma_L^2}\right)}{2h_i\sqrt{2\pi\sigma_L^2}}, \quad h_i > 0. \tag{56}$$

Now, following the similar derivation methodology of scenario 1, the closed-form expression corresponding to the ABER of scenario 2 is given by:

$$\text{ABER} = \text{abs}\Big(\frac{b}{4\pi}(P_2 - P_3)\Big). \tag{57}$$

A closed-form expression corresponding to P_2 is given as:

$$P_2 = b\Big[\text{erfc}(s) - \frac{s\text{ExpIntegralE}[\frac{1}{2}(1+\frac{1}{b^2}), s^2]}{\sqrt{\pi}}\Big], \tag{58}$$

Table II
SIMULATION PARAMETERS FOR THE PROPOSED V2V-VLC MODEL [22,13]

Parameter	Value
W_L	5 m
W_v	2.5 m
σ_L^2	0.8
σ_i	1
η	1
P_t	10 W
n_d	10
p	0.5
d	20 m (ABER corresponding to scenario 1)
d_h	2 m (ABER corresponding to scenario 2)
D_R	5 cm
Ψ	180°

where $s = h_{2,\text{Eff}}^{PL}\ e^{-2\sigma_L^2}\sqrt{\frac{\gamma_i}{2}}$. Further, a closed-form expression corresponding to P_3 is expressed as:

$$P_3 = sbe^{-s^2} \times \frac{\left(2b^2 - \left(1 + (-1 + 2s^2)\right)b^2 e^{s^2}\text{ExpIntegralE}[\frac{1}{2}(-1 + \frac{1}{b^2}), s^2]\right)}{2(-1 + b^2)\sqrt{\pi}}. \tag{59}$$

As far as the diversity order is concerned, following the similar technique as adopted for scenario 1, the diversity order corresponding to scenario 2 is also obtained as $d_o = 2$.

V. RESULTS AND DISCUSSION

In this section, we will present and discuss the numerical results derived in the previous sections. We perform Monte Carlo simulations to validate our derived results. Note that weather conditions have a significant impact on the outdoor V2V-VLC system. To this end, different performance metrics such as path loss, outage probability, ABER, and diversity property under different weather conditions are going to be a vital part of our discussion. All the simulation parameters related to the proposed V2V-VLC model are well tabulated in Table II.

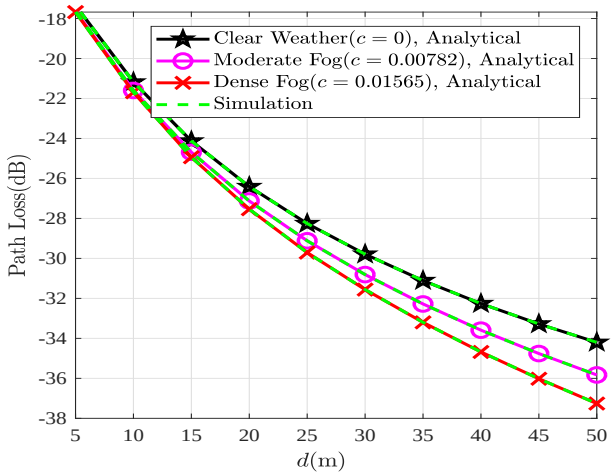

Figure 2. Effect of path loss on the proposed V2V-VLC model corresponding to scenario 1.

A. Effect of Path Loss (Scenario 1)

In this subsection, we reflect an interesting insight into the effect of path loss on the proposed V2V-VLC model corresponding to scenario 1. Since LED-based VLC is mainly intended for short-distance communications, the effect of path loss on the V2V-VLC is significant. In Fig. 2, we plot the path loss curves for different weather conditions and varying distances. We use (20) to plot the path loss curves. For clear weather conditions, we can observe from Fig. 2 that the path loss range lies approximately between -18 to -34 dB for the given distance range. For moderate fog, it is -18 to -36 dB. For dense fog conditions, the path loss range is around -18 to -38 dB.

Observation 1: Differing from the existing literature [29–34], we emphasize the **path loss *penalty*** offered by the considered V2V-VLC system under the ***random*** lateral shift of the vehicle. ***To this end, at a distance of 40 m, for example, the path loss penalties for moderate and dense fog weather scenarios are 2 and 3 dB, respectively compared with the clear weather.*** Therefore, the penalty in terms of the path loss for the considered V2V-VLC system under the random lateral shift of the vehicle is significant.

B. Outage Performance (Scenario 1)

In this subsection, we envision the outage performance of the proposed V2V-VLC model corresponding to scenario 1. In Fig. 3, we plot the outage performance curves for varying distances. We use (26) to plot the outage performance curves. One can observe from Fig. 3, with an increase in the longitudinal separation/transmission distance, the value of the outage probability increases.

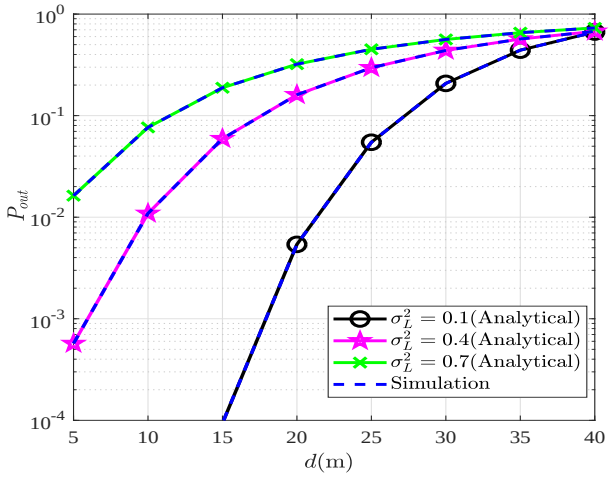

Figure 3. Outage performance of the proposed V2V-VLC model corresponding to scenario 1.

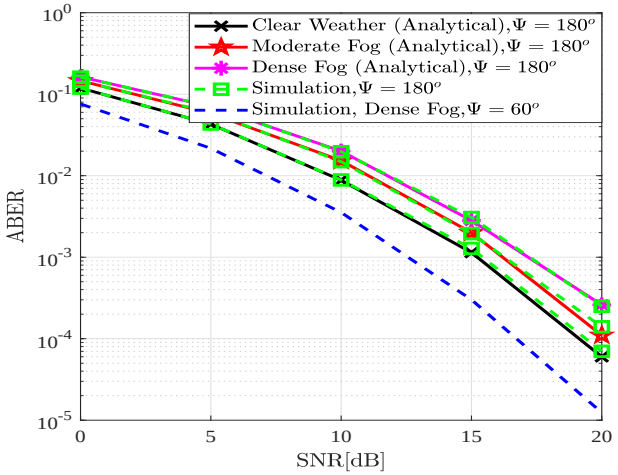

Figure 4. ABER performance of the proposed V2V-VLC model corresponding to scenario 1.

As far as the impact of the σ_L^2 on the outage performance is concerned, the outage performance improves as the value of σ_L^2 decreases. *Note that the considered system performs the best for* σ_L^2 *=0.1.*

C. ABER and Diversity Performance (Scenario 1)

In this subsection, we envision the ABER performance of the proposed V2V-VLC model corresponding to scenario 1. To plot the ABER performance curves corresponding to different weather conditions, we use (41). Fig. 4 illustrates the ABER performance curves of the proposed V2V-VLC model corresponding to different weather conditions for the considered scenario. In Fig. 4, note that the ABER performance curve corresponding to clear weather conditions outperforms the other

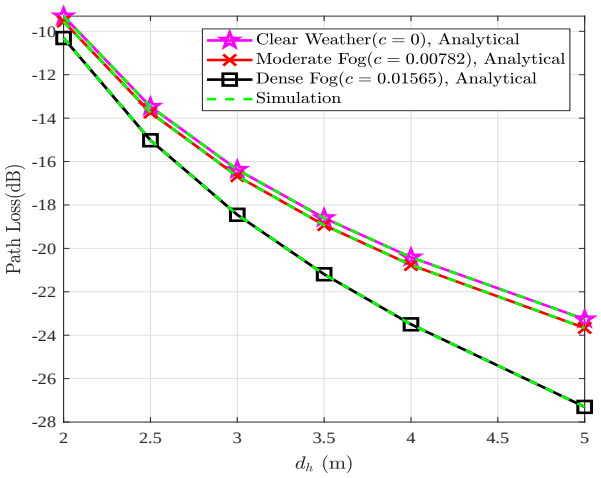

Figure 5. Effect of path loss on the proposed V2V-VLC model corresponding to scenario 2.

ABER performance curves. It shows the impact of weather conditions on the ABER performance of the considered V2V-VLC system. To envision the impact of FOV on the ABER performance, a simulation-based ABER curve corresponding to a dense fog weather scenario with $\Psi = 60^o$ is also presented. It can be observed from the figure that a narrow FOV-based Rx provides a significant performance gain. **Note that a narrow FOV-based Rx captures less noise.** However, this performance gain is valid for specific longitudinal separation of $d = 20$ m (as depicted in Table II). An increase in the value of d along with **random mobility** will decrease the received SNR and eventually deteriorate the ABER of the system.

Let us also reflect some interesting insight into the *diversity* performance of the considered V2V-VLC system. The diversity is the slope of decay of ABER versus SNR plot at asymptotically high values of SNR. *It is worth mentioning that diversity corresponds to the reliability of the communication system. Therefore, the investigation of the diversity property is a vital performance metric of interest.*

Let us calculate the diversity order of the considered scenario corresponding to the moderate fog ABER performance curve. For instance, ABER is 1.488×10^{-2} at 10 dB whereas it is 1.4×10^{-4} at 20 dB and therefore slope can be obtained as $\log_{10}(1.488 \times 10^{-2}/1.4 \times 10^{-4})$, which is approximately equal to 2. *This shows that full diversity of $N_t \times N_r$ is obtained, where N_t and N_r are the number of Txs and Rxs, respectively.* Since the ABER performance curves for all the weather conditions are parallel to each other, diversity is also the same for all three ABER performance curves.

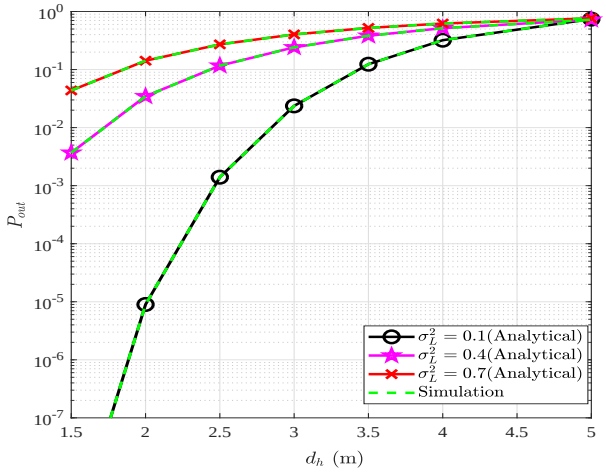

Figure 6. Outage performance of the proposed V2V-VLC model corresponding to scenario 2.

D. Effect of Path Loss (Scenario 2)

In this subsection, we emphasize some useful insights corresponding to the path loss related to scenario 2. In Fig. 5, we plot the path loss curves for different weather conditions and varying lateral shifts. We use (53) to plot the path loss curves. For clear weather, we can observe from Fig. 5 that the path loss range lies approximately between -10 to -24 dB for the given range of lateral shift. For moderate fog, there is a slight deterioration as compared to clear weather. For dense fog conditions, the path loss range is around -10 to -28 dB.

Observation 2: Differing from the indoor VLC, the outdoor V2V-VLC path loss is highly dependent on the weather conditions, ***random*** **lateral movement** of the vehicle, and ***random*** **longitudinal separation** between two communicating vehicles. Now, let us compare the **impact** of path loss of the considered V2V-VLC system corresponding to scenario 1 and scenario 2, illustrated in Fig. 2 and Fig. 5, respectively. *Under different weather scenarios, it can be observed from the figures that the longitudinal separation has more impact on the system performance compared to the lateral shift.* **This conclusion is supported by the fact that for a lane width of** $W_L = 5$ **(depicted in Table II), we have considered a maximum possible range of** d_h **in Fig. 5. Note that,** d **can further be increased, however, it is not practically possible to increase** d_h **further.**

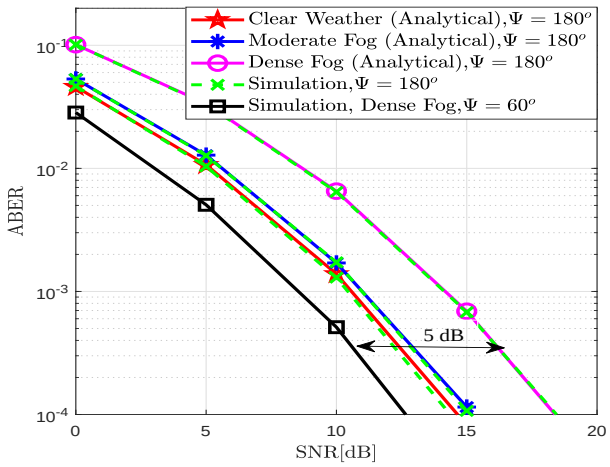

Figure 7. ABER performance of the proposed V2V-VLC model corresponding to scenario 2.

E. Outage Performance (Scenario 2)

In this subsection, we envision the outage performance of the proposed V2V-VLC model corresponding to scenario 2. In Fig. 6, we plot the outage performance curves for varying lateral shifts. We use (55) to plot the outage performance curves. It can be observed from Fig. 6 that with an increase in the lateral shift, the value of the outage probability increases. Similar to scenario 1, the outage performance improves as the value of σ_L^2 decreases.

Observation 3: Differing from the indoor VLC scenario wherein there is no existence of atmospheric turbulence, in this work, the effect of **log-amplitude variance** (σ_L^2) on the outage performance of the outdoor V2V-VLC system is observed. ***Moreover, differing from the existing literature [29–34], random path loss is considered.*** **Therefore, a more realistic observation is marked in this work.** Let us compare the outage performance of scenario 1 (for varying longitudinal separation) and scenario 2 (for varying lateral shifts), depicted in Fig. 3 and Fig. 6, respectively. ***It can be observed that as the value of σ_L^2 increases, the impact of lateral shift becomes more significant compared to the longitudinal separation.***

F. ABER and Diversity Performance (Scenario 2)

In this subsection, we envision the ABER performance of the proposed V2V-VLC model corresponding to scenario 2. Fig. 7 illustrates the ABER performance curves of the considered V2V-VLC system corresponding to different weather conditions for the considered scenario. Similar to scenario

1, we can observe from Fig. 7 that the ABER performance curve corresponding to clear weather conditions outperforms the other ABER performance curves. However, contrary to scenario 1, the ABER performance curves of scenario 2, corresponding to clear weather and moderate fog weather conditions, are almost identical to each other. *It shows that for clear weather and moderate fog-based weather conditions, the longitudinal separation has less impact on the ABER performance.* To envision the impact of FOV on the ABER performance, a simulation-based curve corresponding to a dense fog weather scenario with $\Psi = 60^o$ is also presented. It can be observed from the figure that a narrow-FOV based Rx provides a significant performance gain of 4-5 dB. However, this performance gain is valid for a specific lateral shift/mobility of $d_h = 2$ m (as depicted in Table II). *Note that with a **slight increase** in lateral shift of the vehicle, the Txs will be out of the narrow FOV of Rx, and the ABER performance will deteriorate significantly.* **Therefore, to address the practical constraint of mobility, a wide-FOV-based Rx is generally preferred for a V2V-VLC [22]**.

Let us calculate the diversity order corresponding to the moderate fog ABER performance curve. For instance, ABER is 1.268×10^{-2} at 5 dB whereas it is 1.07×10^{-4} at 15 dB and therefore the slope can be obtained as $\log_{10}(1.268 \times 10^{-2}/1.07 \times 10^{-4})$, which is approximately equal to 2 (i.e., full diversity).

Observation 4: Let us compare the ABER performance corresponding to scenario 1 and scenario 2, as depicted in Figs. 4 and 7, respectively. For example, at an SNR=15 dB with $\Psi = 180^o$ and for dense fog weather conditions, the ABER corresponding to scenario 1 is higher. It shows the **joint impact** of random lateral shift of the vehicle and the deterioration in the weather conditions on the considered V2V-VLC system in terms of the ABER performance.

VI. Conclusions

In this work, a comprehensive V2V-VLC model under practical considerations was proposed, and its performance with different metrics was analyzed. The performance of the proposed V2V-VLC model was investigated under different weather scenarios. Moreover, a novel channel model that takes into account the joint impact of path loss and atmospheric turbulence was considered. *To this end, two realistic V2V-VLC scenarios were considered.* In scenario 1, the random lateral shift of vehicles and the deterministic longitudinal separation between two vehicles were considered,

whereas in scenario 2, longitudinal separation between two vehicles and lateral shift of vehicles were considered to be random and deterministic, respectively. **It was observed, the path loss penalty for the considered V2V-VLC system under the random lateral shift of the vehicle was significant. Further, considering scenario 2, it was observed that under clear weather and moderate fog-based weather conditions the longitudinal separation has less impact on the ABER performance. Furthermore, it was observed that the joint impact of path loss and atmospheric turbulence on the V2V-VLC system is significant.** Finally, the reliability of the considered V2V-VLC system was acknowledged by studying the diversity property.

REFERENCES

[1] S. Dimitrov and H. Haas,"Principles of LED Light Communications: Towards Networked Li-Fi." Cambridge, U.K.: Cambridge Univ. Press, 2015.

[2] L. Yin, W. O. Popoola, X. Wu, and H. Haas, "Performance evaluation of non-orthogonal multiple access in visible light communication," *IEEE Trans. Commun.,* vol. 64, no. 12, pp. 5162-5175, Dec. 2016.

[3] N. Sklavos, M. Huebner, D. Goehringer, and P. Kitsos,"System-Level Design Methodologies for Telecommunication." London, U.K.: Springer, 2014.

[4] P. Sharda and M. R. Bhatnagar, "Diversity-multiplexing tradeoff for indoor visible light communication,"*2020 16th International Conference on Wireless and Mobile Computing, Networking and Communications (WiMob),* pp.1-6, Oct. 2020.

[5] M. Kashef , M. Abdallah, and N. Al-Dhahir,"Transmit power optimization for a hybrid PLC/VLC/RF communication system," *IEEE Trans. Green Commun. Netw.,* vol. 2, no. 1, pp. 234-245, Mar. 2018.

[6] X. Li, R. Zhang, and L. Hanzo,"Cooperative load balancing in hybrid visible light communications and WiFi," *IEEE Trans. Commun.,* vol. 63, no. 4, pp. 1319-1329, Apr. 2015.

[7] A. M. Cailean and M. Dimian,"Current challenges for visible light communications usage in vehicle applications: A survey," *IEEE Commun. Surveys Tuts.,* vol. 19, no. 4, pp. 2681-2703, Fourth Quarter 2017.

[8] H. L. Minh, D. O'Brien, G. Faulkner, L. Zeng, K. Lee, D. Jung, Y. Oh, and E. T. Won, "1000-Mb/s NRZ visible light communications using a postequalized white led,"*, IEEE Photon. Technol. Lett.,* vol.21, no. 15, pp.1063-1065, Aug. 2009.

[9] Y. Tanaka, T. Komine, S. Haruyama, and M. Nakagawa, "Indoor visible communication utilizing plural white LEDs as lighting in,"*Proc. 12th IEEE Int. Symp. Pers., Indoor Mobile Radio Commun.,* Sept./Oct. 2001, vol.2, pp.F-81-F-85.

[10] L. Zeng, D. O'Brien, H. Minh, G. Faulkner, K. Lee, D. Jung, Y. Oh, and E. T.Won, "High data rate multiple input multiple output (MIMO) optical wireless communications using white LED lighting," *IEEE J. Sel. Areas Commun,* vol.27, no. 9, pp.1654-1662, Dec. 2009.

[11] T. Little, P. Dib, K. Shah, N. Barraford, and B. Gallagher, "Using LED lighting for ubiquitous indoor wireless networking," *Proc. IEEE Int. Conf. Wirel. Mobile Comput., Network. Commun.,* Oct. 2008, pp.373-378.

[12] Z. Ghassemlooy, L. N. Alves, S. Zvanovec, and M. A. Khalighi,"Visible Light Communications: Theory and Applications." Boca Raton, FL, USA: CRC Press, 2017.

[13] Z. Ghassemlooy, W. Popoola, and S. Rajbhandari, "Optical Wireless Communications System and Channel Modelling with MATLAB," *CRC Press,* 2013.

[14] J.B. Wang, Q.S. Hu, J. Wang, M. Chen, and J. Wang, "Tight bounds on channel capacity for dimmable visible light communications," *J. Lightwave Tech.,* vol. 31, no. 23, pp. 3771-3779, Oct. 2013.

[15] S.H. Yu, O. Shih, H.M. Tsai, N. Wisitpongphan, and R. D. Roberts, "Smart Automotive Lighting for Vehicle Safety," *IEEE Communications Magazine,* vol. 51, no. 12, pp. 50-59, Dec. 2013.

[16] S. J. Lee, J. K. Kwon, S. Y. Jung, and Y. H. Kwon, "Simulation modeling of visible light communication channel for automotive applications," *15th International IEEE Conference on Intelligent Transportation Systems,* pp. 463-468, 2012.

[17] A. M. Cailean and M. Dimian, "Toward environmental-adaptive visible light communications receivers for automotive applications: A review," *IEEE Sensor Journal,* vol. 16, no. 9, pp. 2803-2811, May 2016.

[18] A. Al-Kinani, J. Sun, C. X. Wang, W. Zhang, X. Ge, and H. Haas, "A 2-D non-stationary GBSM for vehicular visible light communication channels," *IEEE Trans. Wireless Commun.,* vol. 17, no. 12, pp. 7981-7992, Dec. 2018.

[19] M. Elamassie, M. Karbalayghareh, F. Miramirkhani, R. C. Kizilirmak, and M. Uysal, "Effect of fog and rain on the performance of vehicular visible light communications,"*2018 IEEE 87th Vehicular Technology Conference (VTC Spring),* pp.1-6, 2018.

[20] H. Farahneh, F. Hussain, R. Hussain, and X. Fernando, "A novel optimal precoder and equalizer in 2×2 MIMO VLC systems for vehicular application,"*2018 IEEE Globecom Workshops (GC Wkshps),* pp.1-6, 2018.

[21] H. Jiang, Z. Zhang, J. Dang and L. Wu, "A novel 3-D massive MIMO channel model for vehicle-to-vehicle communication environments," *IEEE Trans. Commun.,* vol. 66, no. 1, pp. 79-90, Jan. 2018.

[22] M. Karbalayghareh, F. Miramirkhani, H. B. Eldeeb, R. C. Kizilirmak, S. M. Sait, and M. Uysal, "Channel modeling and performance limits of vehicular visible light communication systems," *IEEE Trans. Veh. Technol.,* vol. 69, no. 7, pp. 6891-6901, Jul. 2020.

[23] E. Eso, S. Teli, N.B. Hassan, S. Vitek, Z. Ghassemlooy, and S. Zvanovec, " 400 m rolling-shutter-based optical camera communications link," Opt. Lett. 45, pp.1059-1062, 2020.

[24] M. R. Soares, N. Chaudhary, E. Eso, O. I. Younus, L. N. Alves, and Z. Ghassemlooy, "Optical camera communications with convolutional neural network for vehicle-to-vehicle links," *2020 12th International Symposium on Communication Systems, Networks and Digital Signal Processing (CSNDSP),* pp.1-6, 2020.

[25] R. Yin, Z. Ghassemlooy, N. Zhao, H. Yuan, M. Raza, E. Eso, and S. Zvanovec "A multi-hop relay based routing algorithm for vehicular visible light communication networks," *2020 12th International Symposium on Communication Systems, Networks and Digital Signal Processing (CSNDSP),* Porto, Portugal, 2020, pp. 1-6.

[26] R. Mitra, F. Miramirkhani, V. Bhatia, and M. Uysal "Low complexity least minimum symbol error rate based post-distortion for vehicular VLC," *IEEE Trans. Veh. Technol.,* vol. 69, no. 10, pp. 11800-11810, Oct. 2020.

[27] C. Huang, R. Wang, P. Tang, R. He, B. Ai, Z. Zhong, C. Oestges and A. F. Molisch, "Geometry-cluster-based stochastic MIMO model for vehicle-to-vehicle communications in street canyon scenarios," *IEEE Trans. Wireless Commun.,* vol. 20, no. 2, pp. 755-770, Feb. 2021.

[28] A. S. Hamza, J. S. Deogun, and D. R. Alexander, "Classification framework for free space optical communication links and systems," *IEEE Commun. Surveys Tuts.,* vol. 21, no. 2, pp. 1346-1382, Second Quarter 2017.

[29] R. W. Zaki, H. A. Fayed, A. Abd El Aziz, and M. H. Aly, "Outdoor visible light communication in intelligent transportation systems: Impact of snow and rain," *Applied Sciences,* vol. 9, no. 24, p. 5453, Dec. 2019.

[30] D. J. Cuba-Zuniga, S. B. Mafra, and J. R. Mejia-Salazar,"Cooperative full-duplex V2V-VLC in rectilinear and curved roadway scenarios," *Sensors,* vol. 20, no. 13, p. 3734, Jul. 2020.

[31] C. Beguni, A. M. Cailean, S. A. Avatamanitei, and M. Dimian,"Analysis and experimental investigation of the light dimming effect on automotive visible light communications performances," *Sensors,* vol. 21, no. 13, p. 4446, Jun. 2021.

[32] W. Shen and H. Tsai, "Testing vehicle-to-vehicle visible light communications in real-world driving scenarios," *2017 IEEE Vehicular Networking Conference (VNC),* 2017, pp. 187-194, doi: 10.1109/VNC.2017.8275596.

[33] M. Seminara, T. Nawaz, S. Caputo, L. Mucchi and J. Catani "Characterization of field-of-view in visible light communication systems for intelligent transportation systems," *IEEE Photonics Journal,* vol. 12, no. 4, pp. 1-16, Aug. 2020, Art no. 7903816, doi: 10.1109/JPHOT.2020.3005620.

[34] T. Nawaz, M. Seminara, S. Caputo, L. Mucchi, F. S. Cataliotti and J. Catani "IEEE 802.15.7-Compliant ultra-low latency relaying VLC system for safety-critical ITS," *IEEE Trans. Veh. Technol.,* vol. 68, no. 12, pp. 12040-12051, Dec. 2019, doi: 10.1109/TVT.2019.2948041.

[35] A. P. Prudnikov, Y. A. Brychkov, and O. I. Marichev,"Integrals and Series." *Gordon and Breach,* vol. 3, 1990.

[36] T. Komine, J. H. Lee, S. Haruyama, and M. Nakagawa, "Adaptive equalization system for visible light wireless communication utilizing multiple white LED lighting equipment,"*IEEE Trans. Wireless Commun.,* vol. 8, no. 6, pp. 2892-2900, June 2009.

[37] [Online]. Available: reference.wolfram.com/language/ref/ExpIntegralE.html

[38] E. Bayaki, R. Schober, and R. K. Mallik,"Performance analysis of MIMO free-space optical systems in gamma-gamma fading," *IEEE Trans. Commun.,* vol. 57, no. 11, pp. 3415 - 3424, Nov. 2009.

[39] S.G. Wilson, M. B. Pearce, Q. Cao and M. Baedke,"Optical repetition MIMO transmission with multipulse PPM," *IEEE J. Sel. Areas Commun.,* vol. 23, no. 9, pp. 1901 - 1910, Sept. 2005.

[40] M. Safari, and M. Uysal, "Cooperative diversity over log-normal fading channels: performance analysis and optimization," *IEEE Trans. Wireless Commun.,* vol. 7, no. 5, pp. 1963 - 1972, May 2008.

[41] [Online]. Available: https://en.wikipedia.org/wiki/Inverse Gaussian distribution